JVI Journals.ASM.org

Recombinant Adeno-Associated Virus Utilizes Cell-Specific Infectious Entry Mechanisms

Marc S. Weinberg,[a] Sarah Nicolson,[a,b] Aadra P. Bhatt,[c] Michael McLendon,[a] Chengwen Li,[a] R. Jude Samulski[a,b]

Gene Therapy Center,[a] Department of Pharmacology,[b] and Department of Microbiology and Immunology,[c] University of North Carolina, Chapel Hill, North Carolina, USA

ABSTRACT

Understanding the entry and trafficking mechanism(s) of recombinant adeno-associated virus (rAAV) into host cells can lead to evolution in capsid and vector design and delivery methods, resulting in enhanced transduction and therapeutic gene expression. Variability of findings regarding the early entry pathway of rAAV supports the possibility that rAAV, like other viruses, can utilize more than one infectious entry pathway. We tested whether inhibition of macropinocytosis impacted rAAV transduction of HeLa cells compared to hepatocellular carcinoma cell lines. We found that macropinocytosis inhibitor cytochalasin D blocked rAAV transduction of HeLa cells (>2-fold) but enhanced (10-fold) transduction in HepG2 and Huh7 lines. Similar results were obtained with another macropinocytosis inhibitor, 5-(*N*-ethyl-*N*-isopropyl) amiloride (EIPA). The augmented transduction was due to neither viral binding nor promoter activity, affected multiple rAAV serotypes (rAAV2, rAAV2-R585E, and rAAV8), and influenced single-stranded and self-complementary virions to comparable extents. Follow-up studies using CDC42 inhibitor ML141 and p21-activated kinase 1 (PAK1) siRNA knockdown also resulted in enhanced HepG2 transduction. Microscopy revealed that macropinocytosis inhibition correlated with expedited nuclear entry of the rAAV virions into HepG2 cells. Enhancement of hepatocellular rAAV transduction extended to the mouse liver *in vivo* (4-fold enhancement) but inversely blocked heart tissue transduction (13-fold). This evidence of host cell-specific rAAV entry pathways confers a potent means for controlling and enhancing vector delivery and could help unify the divergent accounts of rAAV cellular entry mechanisms.

IMPORTANCE

There is a recognized need for improved rAAV vector targeting strategies that result in delivery of fewer total particles, averting untoward toxicity and/or an immune response against the vector. A critical step in rAAV transduction is entry and early trafficking through the host cellular machinery, the mechanisms of which are under continued study. However, should the early entry and trafficking mechanisms of rAAV differ across virus serotype or be dependent on host cell environment, this could expand our ability to target particular cells and tissue for selective transduction. Thus, the observation that inhibiting macropinocytosis leads to cell-specific enhancement or inhibition of rAAV transduction that extends to the organismic level exposes a new means of modulating vector targeting.

Due to its ease of production, persistence in an episomal form, low immunogenicity, and lack of pathogenicity, adeno-associated virus (AAV) is a highly promising and prevalent gene therapy vector. The variety of capsids occurring naturally and evolving in the laboratory setting has resulted in a wide range of cell- and tissue-specific tropisms for the virus, which are being tested as therapeutic vectors for use against a multitude of diseases (1). Clinical observations suggest that an immunological response can mount against transduced cells, for instance, in the liver (2), and as the immunogenic response shows a dose relationship to vector load (3), there also appears to be a vector dose threshold for rAAV delivery prompting a host immune response (4). This putative upper limit on viral load encourages the discovery and use of alternative means to increase viral uptake, transduction, and transgene expression while minimizing viral delivery titers.

Mechanisms to enhance recombinant AAV (rAAV) transduction have emphasized capsid design, where naturally occurring (5–7) or laboratory-based rational design (8–11) and directed evolution-based capsid schemas (12, 13) have yielded dramatic shifts in viral attachment to host cell glycoproteins and protein receptors, conferring differing tissue tropisms and binding efficiencies. Alternative approaches to improve vector transduction and transgene expression have come out of altering the later trafficking ubiquitination and/or proteasomal degradation of rAAV virions (14, 15), affecting nuclear localization signals on the viral capsid (16), avoidance of the rate-limiting step of second-strand DNA synthesis (17), or optimization of the transgene cassette for enhanced translation (18).

Compared with the application of the aforementioned approaches to improve rAAV transduction, less emphasis has been placed on attempting to improve viral entry and early cellular trafficking. This could be due in part to a lack in consensus over the rAAV entry process or to the assumption that entry and early trafficking are universal, fixed processes. Initially, researchers proposed that dynamin- and clathrin-coated pits were at least partially responsible for rAAV entry into HeLa cells (19, 20). Other reports based on HeLa cell studies postulated that a macropinocytosis-based mechanism might be behind rAAV entry and nuclear trafficking (21). Later research using HeLa as well as HEK293 and

Received 7 July 2014 **Accepted** 7 August 2014
Published ahead of print 20 August 2014
Editor: M. J. Imperiale
Address correspondence to R. Jude Samulski, rjs@med.unc.edu.

doi:10.1128/JVI.01971-14

HepG2 cells found no dependence on clathrin-coated pits or macropinocytosis processes for rAAV entry (22). In line with the latter findings, a more recent study has refuted clathrin-mediated endocytosis as an infectious entry pathway and largely ruled out macropinocytosis processes in successful rAAV transduction of HeLa and HEK293 cells, while identifying an alternative infectious entry route through a lipid raft-based mechanism (23).

Based on the diametric data regarding rAAV entry in cells, it has been proposed that rAAV might utilize more than one entry pathway, the extent to which may vary between host cells (22). This possibility is supported by increasing evidence that viruses other than rAAV can utilize more than one independent internalization pathway to enter a given cell host. For instance, reovirus can enter cells via dynamin-dependent or caveola-dependent mechanisms (24). Other parvoviruses have also been found to utilize multiple independent entry pathways in transducing cells. For examples, porcine parvovirus (PPV) can enter cells both via clathrin-mediated and macropinocytosis-mediated mechanisms (25). Returning to rAAV, at least one study has suggested similar phenomenology, demonstrating that rAAV5 can enter cells via both clathrin- and caveola-based pathways and that these pathways may be used in parallel (26). Infectious entry of viruses can also occur through separate mechanisms in different cell hosts. For instance, equine herpesvirus 1 (EHV-1) enters CHO-K1 cells through an endocytic or phagocytic mechanism, whereas it enters equine dermal (ED) or rabbit kidney (RK13) cells by fusion to the cell surface (27). Similarly, dengue virus 2 (DENV-2) enters Vero cells via a clathrin-independent mechanism, whereas the same virus enters A549 cells through a clathrin-dependent mechanism (28). Thus, the possibility exists that rAAV utilizes more than one entry pathway and that this may be host or environmentally dependent. If it were possible to shift the viral internalization mechanism either toward one of greater efficiency or, conversely, away from one less efficient for cellular infectivity, one could ostensibly deliver rAAV which avoids unintended cellular targets and requires lower overall viral load to transduce a given tissue. Moreover, any evidence supporting the possibility for multiple internalization and infectivity pathways could help converge or unify apparent disparities in our current knowledge of rAAV transduction.

Here we present evidence that drugs known to inhibit the macropinocytosis process, from actin remodeling and membrane ruffling to closure, can have opposing effects on rAAV transduction depending on the cell type studied but regardless of rAAV serotype. We found that rAAV transduction of the often-studied HeLa cell is, in line with the current literature, greatly hindered to macropinocytosis-related inhibitors, whereas inversely, the hepatocellular carcinoma line HepG2 shows a substantial enhancement of transduction. The macropinocytosis inhibitors further resulted in *in vivo* enhancement in liver tissue but decreased heart transduction. Thus, we present a novel means of enhancing rAAV transduction through the redirecting of viral entry processes.

MATERIALS AND METHODS

Cell culture and drugs. HEK293 cells were maintained in Dulbecco's modified Eagle medium (DMEM), and HeLa, HepG2, and Huh7 cells were maintained in RPMI 1640. All cells were maintained at 37°C and 5% CO_2, and media were supplemented with 10% heat-inactivated fetal bovine serum, 100 U/ml of penicillin, and 100 g/ml of streptomycin. For imaging experiments, cells were maintained in phenol red-free media for two passages prior to plating. 5-(*N*-Ethyl-*N*-isopropyl)amiloride (EIPA), 5-(*N*,*N*-hexamethylene)amiloride (HMA), benzamil, amiloride, and ML141 (Sigma-Aldrich, St. Louis, MO) were dissolved in dimethyl sulfoxide (DMSO) and maintained at −20°C.

Virus production. Virus was produced in HEK293 cells as previously described (29, 30). Briefly, polyethylenimine "max" (PEI) was used for the triple transfection of the pXR2/pXR2-R585E/pXR8 cap and rep plasmids, the pXX6-80 helper plasmid, and a terminal repeat (TR)-luciferase (Luc) reporter plasmid containing the firefly luciferase transgene flanked by inverted terminal repeats under the control of the chicken beta actin (CBA) promoter. Cells were harvested between 48 and 72 h posttransfection, and virus was purified by cesium chloride ultracentrifugation. After identification of peak fractions by quantitative PCR (qPCR), virus was dialyzed into phosphate-buffered saline (PBS). Titers were calculated by qPCR according to established procedures (29, 30) using a LightCycler 480 instrument and SV40pA primers previously utilized (31). For Cy5-labeled virus, purified rAAV2 was labeled with Cy5 dye (GE Amersham), extensively dialyzed, and examined for purity as previously described (29, 32). Single-stranded and self-complementary rAAV2-CMV-GFP (ssrAAV2-CMV-GFP and scrAAV2-CMV-GFP, respectively) were prepared and verified for purity as described previously (30).

Cell viability analysis. Drug toxicities were evaluated for all cell lines using CellTiter Aqueous One solution (Promega, Madison, WI) after 18 h of incubation with drug. Cell viability was determined relative to that of vehicle-treated cells. With the exception of the log-scaled dose curve, where a wide range of doses were evaluated, selected drug doses resulted in greater than 80% viability after 18 h of incubation with cultured cells (data not shown).

Transduction and transfection studies. Transduction studies were performed similarly to that described previously (16). Eighteen hours prior to experimentation, cells were plated in 24- or 48-well plates precoated in poly-L-lysine (Sigma-Aldrich, St. Louis, MO) for improved cellular adherence at a cell density of 1e5/ml in 10% serum-containing medium. Immediately prior to virus delivery, medium was replaced with that containing the appropriate dilution of drug (in equal DMSO concentrations not exceeding a final concentration of 0.1%) in 0.5% serum-containing medium. Cells were infected with purified rAAV at the designated number of vector genomes (vg) per cell (multiplicity of infection [MOI] of 1e5 vg unless otherwise specified). Medium was removed and replaced with 1× passive lysis buffer (Promega) at 18 h unless otherwise noted. Luciferase activity was measured in accordance with the manufacturer's instructions (Promega) using a Wallac1420 Victor3 automated plate reader. Raw luciferase activity (counts per second) was divided by protein concentration based on Bradford assay (protein assay dye reagent; Bio-Rad, Hercules, CA) and normalized to fold change over same-virus, same-cell type, vehicle-treated groups.

To examine drug effect on promoter activity, a 10-cm^2 plate of HepG2 or HeLa cells (1e5 cells per ml) was PEI transfected with the TR-CBA-Luc plasmid. Twenty-four hours after transfection, cells were split into 24-well plates, such that each well contained a population of equivalently transfected cells. Twenty-four hours later, medium was replaced with drug- or vehicle-containing medium. Finally, 18 h after drug treatment, cells were harvested for relative luciferase activity and protein assay as described above. Drug-treated mock-transfected cells were compared with plasmid-transfected cells and showed no luciferase activity (data not shown).

siRNA knockdown. To examine whether inhibition of the PAK1 pathway affects AAV transduction of HepG2 cells, we transfected small interfering RNA (siRNA) validated for targeting of human PAK1 (si00605696; Qiagen, Valencia, CA) with a target sequence of 5′-TCCAC TGATTGCTGCAGCTAA-3′), or a validated nontargeting siRNA (Dharmacon, Lafayette, CO), with Lipofectamine 2000 (Invitrogen, Long Island, NY) transfection reagent, in accordance with a supplier-provided transfection protocol. Twenty-four hours posttransfection, medium was replaced, and 1e5 vg of AAV2 was added to each well. Cells were harvested 18 h later for luciferase transduction assay and total protein measurement as described above.

For immunoblot verification of knockdown, HepG2 cells were harvested 48 h posttransfection by washing in ice-cold PBS and lysing in a buffer containing 150 mM NaCl, 50 mM Tris-HCl (pH 8), 0.1% NP-40, 50 mM NaF, 30 mM β-glycerophosphate, 1 mM Na_3VO_4, and 1× complete protease inhibitor cocktail (Roche). Equal amounts of proteins were electrophoresed on a 10% SDS-PAGE denaturing gel, followed by transfer onto a Hybond-ECL nitrocellulose membrane (GE Healthcare). The membrane was blocked with 5% fat-free milk for 1 h at room temperature, followed by overnight incubation at 4°C in anti-PAK1 (Cell Signaling; catalog no. 2602) in 5% bovine serum albumin (BSA). Tubulin (Cell Signaling) was used as a loading control. After washing, the membranes were incubated with anti-rabbit IgG-horseradish peroxidase (HRP). Bands were visualized by chemiluminescence.

Binding studies. To determine basal rAAV2 binding to HepG2 cells, cells were plated 18 h previously onto 24-well plates coated with poly-L-lysine. Medium was replaced with ice-cold 10 mM HEPES-buffered RPMI, and rAAV2 was added at ascending MOIs. After 1 h of incubation at 4°C, cells were washed 3 times in ice-cold PBS, and DNA was harvested using a DNA extraction kit (DNeasy blood and tissue kit; Qiagen, Valencia, CA). Relative genome quantification was performed through qPCR, using primers targeted against the viral vector (luciferase; forward, 5′-AAA AGC ACT CTG ATT GAC AAA TAC-3′, and reverse, 5′-CCT TCG CTT CAA AAA ATG GAA C-3′) and primers targeting the cellular genome (human lamin B2; forward, 5′-GTT AAC AGT CAG GCG CAT GGG CC-3′, and reverse, 5′-CCA TCA GGG TCA CCT CTG GTT CC-3′). qPCR conditions were as follows: 1 cycle at 95°C for 10 min and 45 cycles at 95°C for 10 s, 60°C for 10 s, and 72°C for 10 s for acquisition. rAAV binding was reported as genomes per cell, based on the ratio of vector to cellular DNA. As a standard curve was not utilized for binding studies, measurement of genomes per cell is based in arbitrary units (Luc/lamin). To study the drug-induced effect on rAAV binding to cells, cells were treated identically but HepG2 cells were pretreated with drug- or vehicle-containing medium for 18 h, after which drug-containing medium was replaced with ice-cold 10 mM HEPES-buffered medium containing various genome quantities of rAAV2. For drug effect on binding, Luc/lamin values were normalized and denoted as fold difference from the vehicle-treated group treated with the same MOI.

Flow cytometry. HepG2 cells were treated identically to those in luciferase transduction studies and treated with no virus (NV), 1e3, 1e4, or 1e5 vg of ssAAV2-CMV-GFP or scAAV2-CMV-GFP, and 10 μM EIPA or a vehicle. Eighteen hours postransduction, cell images were first captured with an inverted fluorescence microscope using identical capture settings. (For example, a photomicrograph using an MOI of 1e5 vg scAAV2-CMV-GFP is shown in Fig. 6C.) Image capture was followed by trypsinization, filtration at 0.4 μm, and analysis using a Beckman-Coulter CyAn ADP instrument. Enhanced green fluorescent protein (EGFP) fluorescence was measured using a 488-nm excitation laser and 530- to 540-nm emission filter. Values are raw, not normalized. Results shown are a subset of the total findings; peak EGFP detection sensitivity was found at MOIs of 1e5 vg for ssAAV and 1e3 vg for scAAV under the given conditions.

Confocal microscopy. Microscopy was performed similarly to that previously described (29). Briefly, cells were plated onto poly-L-lysine-coated coverslips at 5e4 cells per ml. Eighteen hours after plating cells, growth medium was exchanged with ice-cold HEPES-buffered (10 mM) RPMI medium containing 5e4 vg of Cy5-labeled rAAV. One hour after 4°C incubation with virus, medium was replaced with prewarmed medium containing 10 μM EIPA or a vehicle and then cells were replaced into 37°C incubators. Thirty minutes or 2 h after incubation, cells were fixed with 4% paraformaldehyde for 15 min, followed by mounting using a 4′,6-diamidino-2-phenylindole (DAPI)-containing medium (ProLong Gold; Invitrogen, Long Island, NY). Images were captured on a Zeiss 710 upright laser scanning confocal microscope using a Plan Apochromat 63×/1.40-numerical-aperture oil objective. Image processing of confocal was performed using AutoQuant and Imaris software (UNC Microscopy Services Laboratory). Scale bars in figures represent 10 μm, and mock-treated cells received drug or a vehicle for 2 h prior to fixation. EIPA results in autofluorescence at the same wavelength as DAPI, resulting in much brighter nuclei and some extranuclear staining (33), but it did not lead to any autofluorescence in the far red spectrum (i.e., Cy5; data not shown). Thus, DAPI-channel brightness settings were adjusted *post hoc* to allow for readily comparable images (see Fig. 7A). For Fig. 7B, the dash-outlined portion of the Cy5 channel, including outlined nuclei, were expanded to allow ready comparison of the representative images.

***In vivo* transduction assays.** All mouse experiments were conducted in accordance with the policies of the University of North Carolina at Chapel Hill's Institutional Animal Care and Use Committee. For *in vivo* transduction experiments, female BALB/c mice were used. Drugs were as follows: cytochalasin D (0.5 mg/kg), EIPA (25 mg/kg), or a vehicle (DMSO in equivalent concentration as in the drug-treated group). Cytochalasin D was delivered retro-orbitally along with 1e11 vg of AAV2-CBA-Luc in a 200-μl volume of 1× PBS. EIPA was delivered by intraperitoneal injection to mice 10 min prior to retro-orbital injection (1e11 vg of AAV2-CBA-Luc in 200 μl of PBS). The retro-orbital delivery strategy was chosen based on high interanimal consistency, as demonstrated previously in our laboratory (e.g., see reference 34). One week later, mice were given 150 mg/kg of D-luciferin (Caliper Life Sciences) intraperitoneally, and after 5 min, luminescence was measured using the IVIS-Lumina imaging system (Caliper Life Sciences). Igor Pro 3.0 software was used to quantitate luminescence signals. For tissue-specific analyses, mice were given a lethal dose of tribromoethanol (Avertin), and tissues were extracted and snap-frozen on dry ice. For luciferase activity analysis, tissue was briefly homogenized in 2× passive lysis buffer (Promega) and clarified by centrifugation. Relative luciferase activity was standardized to total protein through Bradford assay and normalized to fold over value for vehicle-treated mice. Tissue genome quantification was performed identically to cellular genome quantification, and values are normalized to fold Luc/lamin over those for vehicle-treated mice.

Graphing and statistics. Data were represented and statistics quantified using GraphPad Prism 6.0 (GraphPad, La Jolla, CA). Error bars in figures represent standard errors of the means. Statistics for studies with two comparison groups were prepared using a two-tailed Student *t* test, and multigroup statistics were calculated by analysis of variance (ANOVA) using Dunnett's multiple-comparison test (GraphPad), where all groups were compared to the same cell line, same virus-treated, vehicle-treated group.

RESULTS

Cytochalasin D enhances rAAV transduction of hepatocellular lines HepG2 and Huh7 but decreases transduction in HeLa cells. Cytochalasin D is a potent actin polymerization inhibitor that prevents initiation of membrane ruffling and thereby blocks macropinocytosis (35). HeLa cells have served as a classic standard cell line for establishing critical steps in viral trafficking for many viruses, including herpesvirus (36), adenovirus (37), and poliovirus (38). More pertinently, HeLa cells have been used as target cells in most recent studies on rAAV entry mechanisms (e.g., see references 19, 21, and 23). HepG2 and Huh7 cells, in contrast to HeLa cells, exhibit a number of phenomena similar to those in their untransformed hepatocellular counterparts (39, 40) and were studied in this work in parallel to HeLa cells in order to examine cell-specific effects. We first performed toxicity studies with cytochalasin D in HeLa, HepG2, and Huh7 cells, and we found that for all doses, viability was greater than 80% (data not shown). In line with previous studies (21, 23), cytochalasin D inhibited rAAV2 transduction of HeLa cells. In this work, we observed dose-dependent inhibition of luciferase activity up to 50% (Fig. 1A), independent of capsid, suggesting that inhibition of actin polymerization is essential for rAAV transduction of these cells. Inversely, HepG2 or Huh7 cells incubated with cytochalasin D showed

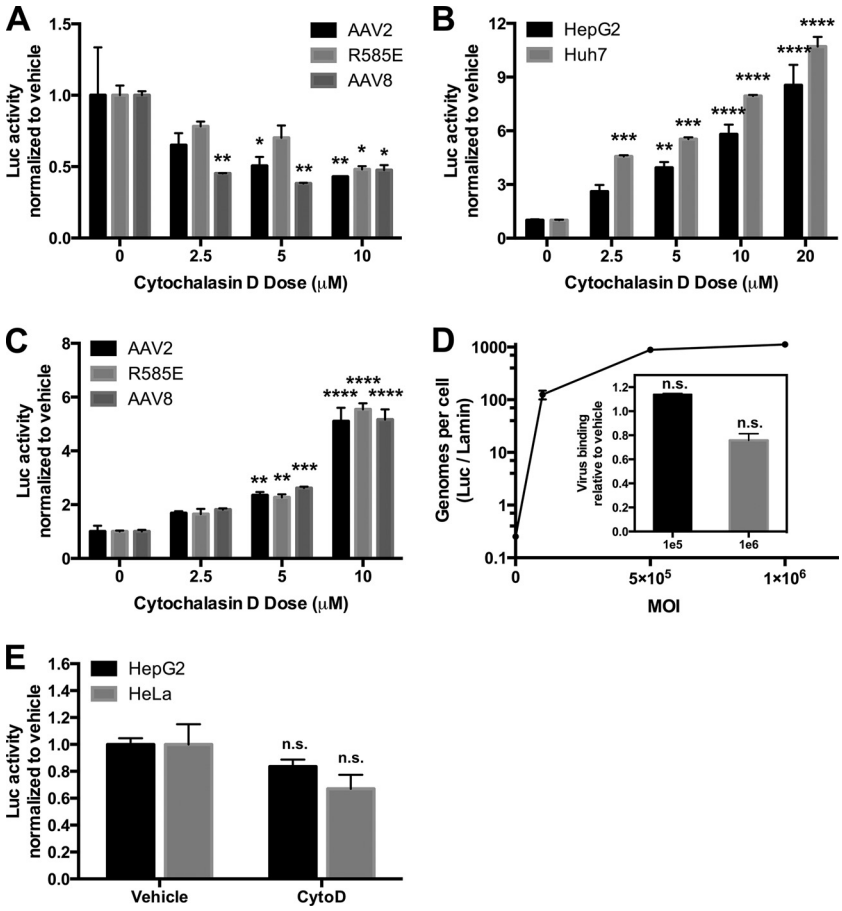

FIG 1 Cytochalasin D enhances AAV transduction of hepatocellular lines. (A) Effect of cytochalasin D on transduction of HeLa cells by alternative AAV serotypes. AAV2, AAV2-R585E (heparin mutant), or AAV8-CBA-Luc (1e5 vg) was delivered to HeLa cells incubating with cytochalasin D at various doses. Eighteen hours after vector delivery, cells were lysed and luciferase activity was determined relative to protein content. (B) Dose-dependent enhancement of AAV2 transduction in HepG2 and Huh7 cells by cytochalasin D. (C) Effect of cytochalasin D on transduction of HepG2 cells by alternative AAV serotypes. (D) Effect of cytochalasin D on AAV2 binding to HepG2 cells. AAV2 at various MOIs was incubated with HepG2 cells at 4°C for 1 h, after which time cells were washed and DNA was extracted. AAV genomes were compared to a cellular housekeeping gene by qPCR. (Inset) A binding study was performed using two AAV MOIs on HepG2 cells preincubated for 18 h with cytochalasin D (10 μM) or a vehicle, and genomes per cell were compared between drug- and vehicle-treated cells. (E) Effect of cytochalasin D on expression of a transfected reporter plasmid. HepG2 and HeLa cells were transfected with pTR-CBA-Luc, and 48 h later, cells were treated with cytochalasin D (10 μM) for 18 h, followed by cell harvest and luciferase activity/protein quantification. Error bars represent standard errors. Statistical significance was determined using ANOVA (Dunnett's multiple-comparison test) or *t* test, comparing drug- to vehicle-treated groups. *, $P < 0.05$; **, $P < 0.01$; ***, $P < 0.001$; ****, $P < 0.0001$. n.s., nonsignificant.

a dose-responsive enhancement of rAAV2 transduction of ~10-fold (Fig. 1B), indicating that blocking the macropinocytosis pathway is conducive to rAAV trafficking in these cells. The dose-responsive enhancement of transduction extended to rAAV2-R585E (heparin-binding-deficient capsid [41]) as well as rAAV8 (Fig. 1C), demonstrating that the effectiveness of these drugs is not related to viral receptor targeting. To test whether the enhancement of HepG2 transduction was due to increased viral binding to the cell surface, we first determined the saturating MOI of rAAV2 on HepG2 cells by performing a binding curve of the cells at 4°C with ascending viral MOIs (Fig. 1D). The quantity of 5e5 vg was determined as a saturating MOI, as doubling the MOI to 1e6 vg did not increase binding. We next incubated cells in a vehicle or cytochalasin D (10 μM) for 18 h, followed by binding of rAAV2 at nonsaturating (1e5 vg) and saturating (1e6 vg) doses of rAAV at 4°C. Incubation in the drug did not alter rAAV binding to HepG2 cells at either MOI (Fig. 1D, inset). We next evaluated whether the drug altered promoter activity by transfecting HepG2 and HeLa cells with pTR-CBA-Luc (Fig. 1E). Two days post-transfection, cells were treated with a vehicle or cytochalasin D (10 μM) for 18 h and harvested for luciferase and protein assay. There was no significant difference in luciferase activity from cytochalasin D-treated HepG2 or HeLa cells, suggesting that the drug was likely not acting on the transgene promoter to influence luciferase activity.

Notably, while all data are reported in fold differences from no-drug group for clarity and visibility, there was approximately a 10-fold decrease in absolute luciferase expression in either HeLa or HepG2 cells when infected with rAAV2-R585E or rAAV8 compared with rAAV2 and, similarly, a 10-fold decrease in absolute luciferase expression in HepG2 cells compared to HeLa cells in the absence of drug treatment.

The macropinocytosis inhibitor EIPA enhances rAAV transduction of HepG2 cells. Having demonstrated that the actin polymerization inhibitor cytochalasin D could potently enhance rAAV transduction in two hepatocyte-derived cell lines but decreased transduction of HeLa cells, we wanted to confirm that the transduction-enhancing actions of cytochalasin D were based in

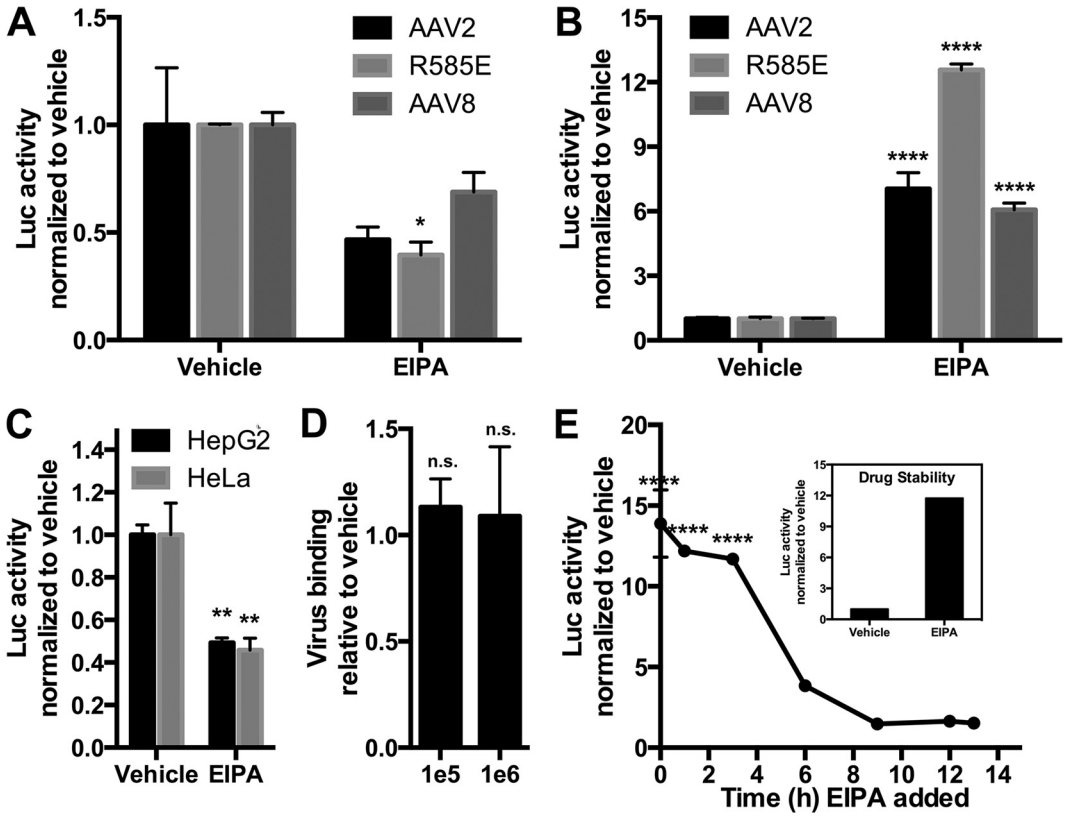

FIG 2 EIPA enhances AAV transduction of hepatocellular lines. (A and B) Effect of EIPA on transduction of HeLa cells (A) or HepG2 cells (B) by alternative AAV serotypes. AAV2, AAV2-R585E (heparin mutant), or AAV8 (1e5 vg) was delivered to cells incubating with EIPA (10 μM). Eighteen hours after vector delivery, cells were lysed and luciferase activity was determined relative to protein content. (C) Effect of EIPA on expression of a transfected reporter plasmid. HepG2 and HeLa cells were transfected with pTR-CBA-Luc, and 48 h later, cells were treated with vehicle or EIPA (10 μM) for 18 h, followed by cell harvest and luciferase activity/protein quantification. (D) Effect of EIPA on AAV2 binding to HepG2 cells. HepG2 cells pretreated with a vehicle or EIPA (10 μM for 18 h) were incubated at 4°C with AAV2 at 1e5 or 1e6 vg for 1 h, after which time cells were washed and DNA extracted. AAV genomes were compared to a cellular housekeeping gene through qPCR. (E) EIPA (10 μM) was given to HepG2 cells at various time points after providing AAV2-CBA-Luc (1e5 vg). Cells were harvested at 14 h after AAV delivery, and luciferase activity/protein content was determined. (Inset) EIPA aliquot used for the time course study was posttested for drug stability by treating HepG2 cells with or without the drug in the presence of AAV2. Cells were harvested and luciferase activity/protein content was determined. Error bars represent standard errors. Statistical significance was determined using ANOVA (Dunnett's multiple-comparison test) or *t* test, comparing drug- to vehicle-treated (and virus-treated) groups. *, $P < 0.05$; **, $P < 0.01$; ****, $P < 0.0001$. n.s., nonsignificant.

its effect of inhibiting macropinocytosis and not on the myriad independent effects this drug has on cells. We therefore used another common macropinocytosis-inhibiting drug, 5-(*N*-ethyl-*N*-isopropyl)amiloride (EIPA). EIPA is thought to inhibit macropinocytosis by inducing accumulation of protons in the forming membrane ruffle, altering submembranous pH and acidifying the pH-sensitive actin-remodeling GTPases, such as CDC42, that support membrane ruffling (35, 42). Here, as with cytochalasin D, a toxicity study was performed, and all doses resulted in greater than 80% viability (data not shown). As with cytochalasin D, at a dose of 10 μM EIPA, we found a serotype-independent ~30 to 50% decrease in transduction of these cells (Fig. 2A), as opposed to a serotype-independent enhancement (~6- to 13-fold) of rAAV transduction of HepG2 cells (Fig. 2B). Separately, we tested the effects of EIPA on rAAV transduction of HEK293 cells and, like with HeLa cells, observed a profound inhibition of rAAV transduction in these cells (data not shown). We next transfected HepG2 and HeLa cells with pTR-CBA-Luc and 48 h later incubated cells in a vehicle or EIPA (10 μM) for 18 h. We found a substantial decrease (~55%) in expression of the transgene (Fig. 2C). As there was no toxicity associated with the transfection-drug combination, and as we delayed the use of macropinocytosis inhibitors until 48 h posttransfection to avoid interference with transfection processes, our data suggest that the enhancing effect of EIPA on rAAV transduction of HepG2 cells is not due to effects on promoter activity; rather, luciferase activity likely underestimates the transduction-enhancing effects of EIPA due to the drug's negative effects on promoter function. Second, the data suggest that the decreased HeLa transduction profile by rAAV may be at least partly driven by transcriptional inhibition by this drug. Thus, it is unclear whether EIPA inhibits promoter activity alone or in fact affects transduction of rAAV in HeLa cells as does cytochalasin D. By performing a binding study akin to that with cytochalasin D, we found that there was no effect of EIPA on rAAV binding to HepG2 cells (Fig. 1D). Next, we captured the time window of action of EIPA on enhancing rAAV transduction in HepG2 cells. For this study, we incubated HepG2 cells with rAAV2 (1e5 vg) for 1 h at 4°C and then washed off virus-containing medium, replacing it with warmed media. Thereafter, at various time points after medium replacement (starting immediately at 0 h), we added EIPA to a final concentration of 10 μM and allowed cultures to incubate for a total of 14 h at 37°C. We found that the

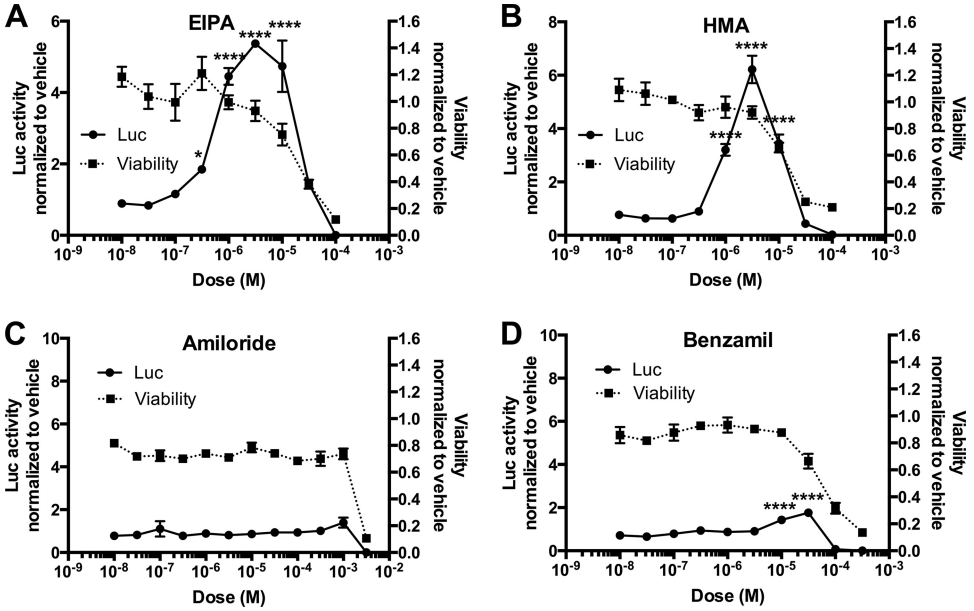

FIG 3 AAV transduction enhancement and toxicity of amiloride analogues on HepG2 cells. HepG2 cells were treated with amiloride analogues EIPA (A), HMA (B), amiloride (C), or benzamil (D) over a log dose scale along with AAV2-CBA-Luc (1e5 vg). Eighteen hours after vector delivery, cells were lysed and luciferase activity was determined relative to protein content (left *y* axis). Separate HepG2 cells were incubated in the presence of the drugs to determine cell viability via MTS assay (right *y* axis). Error bars represent standard errors. Statistical significance was determined using ANOVA (Dunnett's multiple-comparison test), comparing drug- to vehicle-treated groups. *, $P < 0.05$; ****, $P < 0.0001$.

enhancing effects of EIPA on rAAV transduction were retained fully up until at least 3 h postbinding (Fig. 2E), throughout which time an ~12- to 14-fold enhancement of transduction was observed. Waiting 6 h to add EIPA after placing rAAV-bound cells at 37°C, the enhancement effect was diminished to ~4-fold enhancement, and waiting beyond 6 h to add the drug led to no discernible change in transduction from untreated cells. To maintain internal consistency in the time course study, the same aliquot of concentrated drug was used throughout the study. To verify the functionality of the drug over the entire testing period, we added a sample of this aliquot (or a vehicle) to a separate set of HepG2 cells with 1e5 vg of rAAV2 after the 14-h study was completed. The drug showed transduction enhancement (~12-fold enhancement) (Fig. 2E, inset) similar to that observed in the time course study.

Amiloride analogues suggest NHE inhibition as the mechanism of enhanced rAAV transduction in HepG2 cells. In planning an *in vivo* follow-up of the chemical inhibition studies performed on HepG2 and HeLa cells, we found little literature support for the use of EIPA or cytochalasin D beyond basic *in vitro* research purposes. However, the drug from which EIPA was derived, amiloride, has a solid history of previous human use in clinical trials (43–46). Thus, should this drug show transduction enhancement properties similar to those of EIPA, it would be a stronger candidate for *in vivo* testing. Amiloride dually targets the Na^+/H^+ exchangers (NHEs) and epithelial Na^+ channel (ENaC). HepG2 cells utilize ENaC (47) as well as NHEs (48, 49), and amiloride analogues have been produced that more potently and selectively target one or the other channel. EIPA and 5-(*N*,*N*-hexamethylene)amiloride (HMA) both target NHEs but not ENaC, whereas benzamil potently blocks ENaC but not NHEs (50). We performed an assay of each of these drugs on rAAV transduction of HepG2 cells over a multilog dose range (Fig. 3) and found that the NHE-targeting amiloride analogues EIPA and HMA equally enhanced rAAV transduction of HepG2 cells (Fig. 3A and B), whereas the far weaker NHE inhibitor amiloride and ENaC-specific inhibitor benzamil had a limited to no effect on transduction (Fig. 3C and D). Thus, the transduction-enhancing effects of EIPA likely occur through NHE inhibition, suggesting that amiloride is not a comparable alternative to EIPA for *in vivo* testing of rAAV enhancement.

Cytochalasin D and EIPA enhance liver transduction *in vivo*. Whether the enhanced rAAV transduction of hepatocyte-like cells by macropinocytosis inhibitors is strictly an *in vitro* phenomenon or rather extends to the whole organism may help determine the direction and significance of these observations toward further research and clinical value. Thus, the two drugs were independently tested for the ability to enhance transduction in the mouse. Due to limited previous study of these drugs *in vivo*, and the inadequacy of more commonly used amiloride on enhancement of rAAV transduction in cell culture (Fig. 3C), we first performed a dose treatment of mice with the drugs, matching closely the concentrations used in culture to blood concentrations, within the constraints of liver toxicology reports (data not shown). Based on these factors we chose the doses of 0.5 mg/kg of cytochalasin D and 25 mg/kg of EIPA. For cytochalasin D, we simultaneously injected the drug and rAAV2 (1e11 vg) retro-orbitally. For EIPA, to match previous studies using the intraperitoneal (i.p.) route of drug administration (51, 52), we delivered the drug i.p. and followed this with retro-orbital delivery of rAAV2 (1e11) 10 min later. One week later, we analyzed mice for luciferase activity using *in vivo* imaging, and we observed a dominant liver-specific expression pattern expected with the rAAV2 capsid (53), with significantly enhanced luciferase activity in the drug-treated versus vehicle-treated groups (Fig. 4A to C). Notably, the retro-orbital delivery of rAAV2 led to strong luciferase expression in the head region of the mouse. These expression patterns match previous data from our

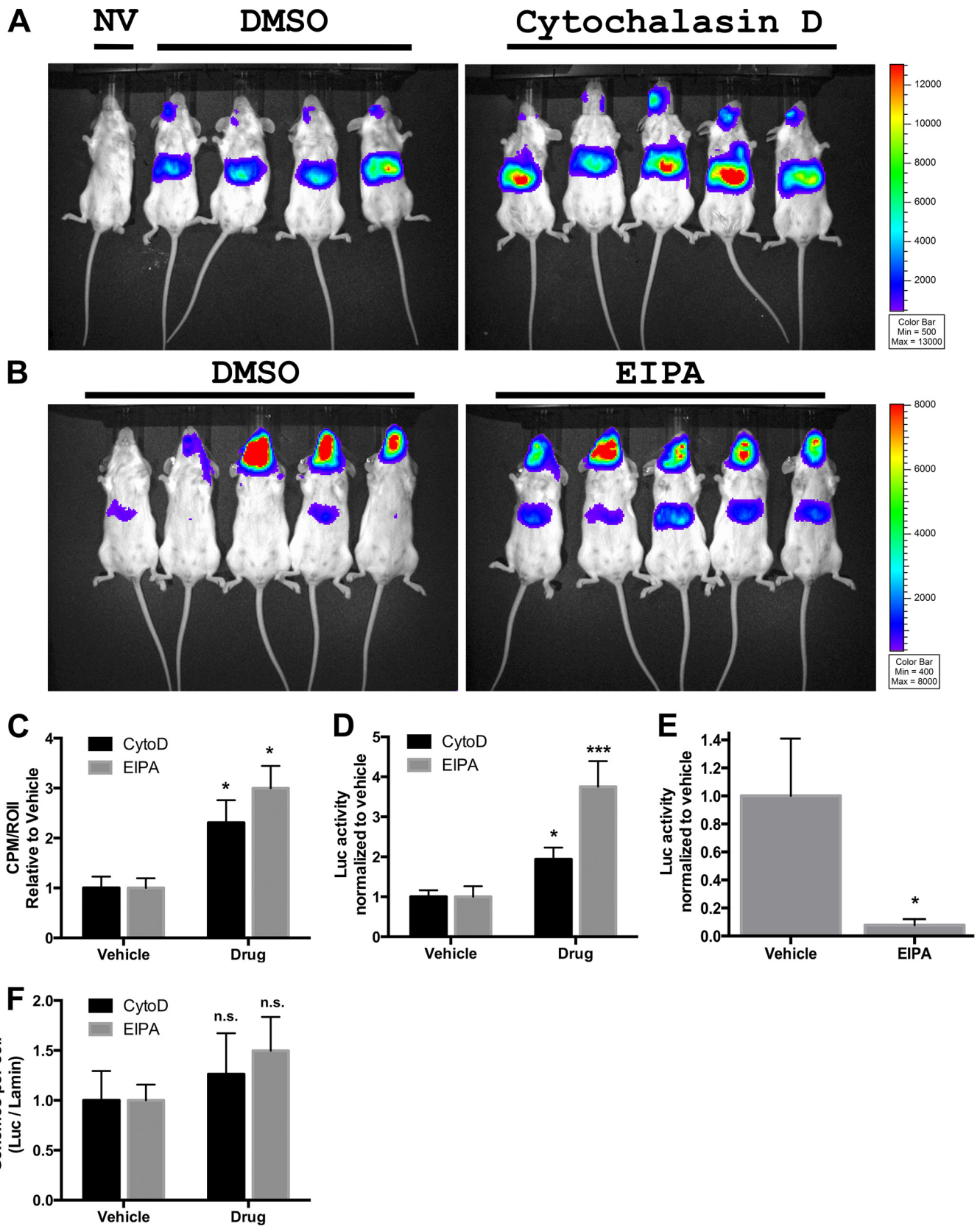

FIG 4 Effect of macropinocytosis inhibitors on liver transduction *in vivo*. Vehicle/cytochalasin D (A) or EIPA (B) was injected into mice along with AAV2-Luc (1e11 vg), and 1 week later, luciferase expression was evaluated by whole-body imaging with a 5-min exposure, using a Xenogen IVIS-Lumina system. (C) Luciferase activity based on Lumina detection was quantified using IVIS-based software. (D) Liver tissue was isolated from mice and homogenized, and luciferase activity was determined relative to protein content. (E) Heart tissue was isolated from mice treated with DMSO or EIPA, and luciferase activity was determined relative to protein content. (F) DNA was extracted from liver tissue, and qPCR analysis quantified AAV genomes versus a cellular housekeeping gene. Statistical significance was determined using *t* test. *, $P < 0.05$; ***, $P < 0.001$. n.s., nonsignificant.

laboratory (34) and are indicative of the delivery methodology and not a shift in tropism of rAAV2 to tissue such as brain. We extracted and homogenized liver tissue and performed a luciferase assay, controlling for protein loading with a Bradford assay. Again we observed a significant increase in liver luciferase activity using either drug (~2-fold increase with cytochalasin D and ~4-fold increase with EIPA) relative to that with the vehicle (Fig. 4D). We also isolated heart tissue from mice in the EIPA treatment study, and a luciferase assay found a strong (90%) decrease in luciferase activity relative to protein content in EIPA-treated mice (Fig. 4E). This EIPA-induced inhibition of rAAV2 transduction in the heart was the opposite of the effect we observed in mouse liver or HepG2 cells and was similar to the inhibitory effect of EIPA on HeLa cell transduction. Beyond liver and heart, we performed additional luciferase analyses with tissue of EIPA-treated mice, including striated muscle and lung, but in these tissues found no drug-related differences in rAAV transduction. As the drug delivery was systemic and not limited to liver and heart tissue, this suggests that the effects of macropinocytosis inhibitors are indeed tissue specific, inducing enhancement, inhibition, or no effect on rAAV transduction depending on the tissue. We further extracted DNA from liver tissue and performed qPCR on the DNA, quantifying vector genomes against a housekeeping gene. We found no significant difference in total virions per cell between drug (either cytochalasin D or EIPA) and vehicle (Fig. 4F). Thus, the drug-induced increase in liver rAAV transduction *in vivo* mirrors our observations with hepatocyte-based cell lines, and like our *in vitro* data, the effects of macropinocytosis inhibitors were found to be cell and tissue specific. Still, the quantifications of rAAV genomes in liver tissue did not differ between drug treatments. This led to the question of how the macropinocytosis inhibitors were prompting such differences in transduction by rAAV in cells.

CDC42 inhibitor ML141 and PAK1 knockdown enhance rAAV transduction in HepG2 cells. In order to begin understanding the mechanism of macropinocytosis inhibitor enhancement of AAV transduction in HepG2 cells, we prepared a transduction experiment *in vitro* utilizing drugs and molecular targets for specific aspects of the macropinocytosis pathway. First we tested the potent, selective CDC42 inhibitor ML141. CDC42 is a member of the Rho family of GTPases and is a key regulator of the actin cytoskeleton, functioning in the formation of filopodia (54) and in the processes leading to membrane ruffling (55). Thus, the noncompetitive, reversible CDC42 inhibitor ML141 was hypothesized to act similarly to the general macropinocytosis inhibitor drugs in enhancing HepG2 transduction. In line with this hypothesis, we found that a 10 μM dose was sufficient to significantly increase luciferase activity in HepG2 cells (Fig. 5A), whereas the same drug inversely led to a dose-dependent decrease in rAAV transduction in HeLa cells (data not shown). These data reveal that inhibition of CDC42 using ML141 recapitulates the effects of the two more generalized macropinocytosis inhibitors. We further followed up the CDC42 inhibitor study by testing whether knockdown of p21-activated kinase 1 (PAK1) would enhance rAAV transduction of HepG2 cells. PAK1 is the downstream effector molecule of Rho GTPase signaling and stimulates cytoskeletal reorganization such as membrane ruffling (56). We transfected HepG2 cells with a manufacturer-validated, well-supported (57, 58) siRNA against PAK1 and compared the effect of knockdown of this protein on AAV transduction to that of a nontargeting siRNA control or mock transfection. As Fig. 5B shows, the PAK1 siRNA but not mock or nontargeting siRNA greatly diminished PAK1 protein levels in HepG2 cells. As for PAK1 knockdown on AAV transduction, transfection of a nontargeting siRNA did not affect rAAV2 transduction of the cells compared to mock treatment, whereas PAK1 knockdown led to >10-fold enhancement of rAAV2 in HepG2 cells (Fig. 5C). Thus, inhibition of macropinocytosis through CDC42 inhibition or PAK1 knockdown can enhance AAV transduction of HepG2 cells.

Effect of EIPA on self-complementary rAAV transduction. In a follow-up study on the mechanism of EIPA on rAAV transduction, we next tested whether the effect of EIPA on rAAV transduction related to an effect of second-strand DNA synthesis on the single-stranded viral genome, a mechanism that other rAAV transduction-enhancing drugs such as hydroxyurea (59) are thought to exploit. To test this possibility, we prepared single-stranded and self-complementary rAAV2-CMV-GFP (ssrAAV2-CMV-GFP and scrAAV2-CMV-GFP, respectively). We verified the purity of self-complementary and single-stranded viral genomes using alkaline gel electrophoresis and Southern blotting (data not shown) and treated HepG2 cells with ssAAV or scAAV at MOIs of 1e3, 1e4, and 1e5 vg in a manner consistent with our previous experiments (18 h of incubation with a vehicle or EIPA at 10 μM). Eighteen hours later, cells were imaged on a fluorescence microscope and then dissociated and analyzed for GFP expression using flow cytometry. We observed an enhancing effect of EIPA on both mean fluorescent activity and percent GFP-positive cells with both ssAAV and scAAV (Fig. 6). EIPA certainly did not have a diminished effect on scAAV transduction compared to ssAAV. Thus, the enhancing effect of EIPA was found to be unrelated to the process of second-strand DNA synthesis of the viral genome. As our studies thus far had found comparable transduction-enhancing effects of three independent macropinocytosis inhibitors and ruled out drug effects on cell binding, promoter activity, second-strand DNA synthesis, or virion accumulation in target tissue, we next sought to visually examine viral localization in cells treated with such drugs, to identify any overt differences in intracellular trafficking patterns.

EIPA enhances early nuclear entry of rAAV in HepG2 cells. To determine whether we could observe overt differences in intracellular trafficking of rAAV in EIPA and vehicle-treated HepG2 cells, we Cy5 labeled AAV2-CBA-Luc and incubated the virus with HepG2 cells at 4°C for 1 h, after which virus-containing medium was replaced with vehicle- or EIPA-containing warmed medium. Thirty minutes or 2 h later, cells were paraformaldehyde fixed and mounted, and confocal microscopy was used to look for the presence of Cy5-labeled virions in the DAPI-labeled nucleus. There was very little background fluorescence in the Cy5 channel, as seen in mock (no virus)-treated cells (Fig. 7A). However, we found a clear qualitative increase in intranuclear Cy5 particles as early as 30 min postincubation, where there were very few Cy5 particles in the nuclei of vehicle-treated cells. After 2 h of incubation, a similar and more extensive enhancement of intranuclear Cy5 signal was observed in the EIPA-treated cells (Fig. 7A), compared with only moderate intranuclear accumulation of particles in the nuclei of vehicle-treated cells. The images of intranuclear Cy5 in virus-treated cells are enlarged (dashed outline represents the enlarged area of Fig. 7A) in Fig. 7B, for better visualization of Cy5-labeled particles. Our microscopy data therefore suggest that the increased rAAV transduction in HepG2 cells treated with macropinocytosis inhibitors is due to rapid trafficking of virus into the

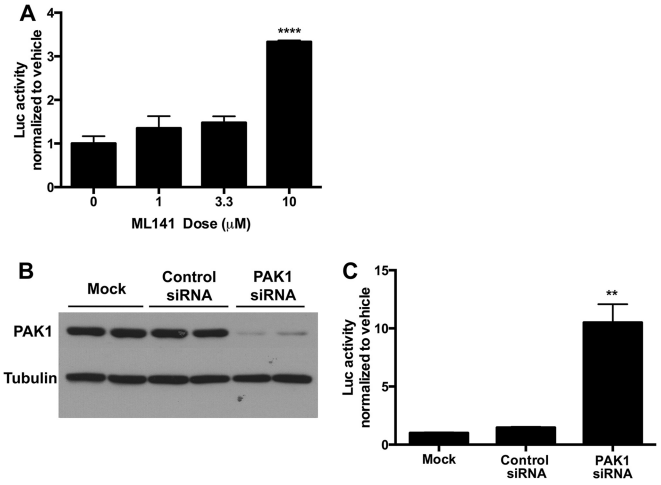

FIG 5 CDC42 inhibition and PAK1 knockdown enhances rAAV transduction of HepG2 cells. (A) HepG2 cells were treated with CDC42 inhibitor ML141 at various doses along with AAV2-CBA-Luc (1e5 vg). (B and C) HepG2 cells were either left untreated or transfected with control or PAK1 siRNA. Forty-eight hours later, cells were harvested for SDS-PAGE and Western blotting against PAK1 and loading control (B), or 30 h later cells, were treated with 1e5 MOI AAV2-CBA-Luc (C). For both ML141 and PAK1 knockdown experiments, 18 h after vector delivery, cells were lysed and luciferase activity was determined relative to protein content. Error bars represent standard errors. Statistical significance was determined using ANOVA. **, $P < 0.01$; ****, $P < 0.0001$.

nucleus, an anticipated outcome considering the demonstrated lack of effect of the macropinocytosis inhibitors on either viral binding or intranuclear processing.

DISCUSSION

In this study, we found through *in vitro* viral infectivity assays that macropinocytosis inhibitors affect rAAV transduction in a cell-specific manner, augmenting infectious entry of hepatocellular lines while inhibiting that of HeLa cells. Neither viral binding to the cell surface nor effects on promoter activity could account for the enhancement of HepG2 transduction, nor is this effect related to second-strand synthesis of the viral genome. While cell dependent, the effects of macropinocytosis inhibition on rAAV transduction were not serotype specific, as three rAAV variants—rAAV2, rAAV2-R585E, and rAAV8—all showed similar transduction profiles. Three independently acting chemical inhibitors of macropinocytosis—cytochalasin-D, EIPA, and ML141—enhanced HepG2 transduction by rAAV while inhibiting HeLa transduction. Further, knockdown of PAK1 confirmed our pharmacological data in demonstrating that macropinocytosis inhibition indeed enhances HepG2 transduction by rAAV. The enhanced transduction appears related to increased efficiency of viral nuclear entry, extended to an additional hepatocellular line (Huh7) in culture, and extended to *in vivo* augmentation of liver cells. However, the *in vivo* enhancement of rAAV transduction was, like *in vitro* data suggested, cell type specific, as heart tissue showed pronounced inhibition of transduction, while other tissue showed no change in rAAV transduction in the presence of macropinocytosis inhibitors.

Classical studies largely performed with HeLa cells provided strong evidence for rAAV entry occurring via a clathrin-mediated mechanism (19, 20), but additional data have secondarily conferred a role for macropinocytosis-related processes on infectious entry in such cells (23), and more recently a study has discounted both clathrin- and macropinocytosis-mediated mechanisms in the infectious entry pathway of rAAV (23). It is challenging to account for such diametric findings between these studies and integrate such findings into a cohesive mechanism for rAAV early trafficking. Perhaps a more cohesive, unified account of rAAV trafficking can be found in the subtler details of the previous studies. For instance, within the context of previous works there is support for multiple rAAV entry pathways: in one study the clathrin-mediated entry inhibitor dynasore significantly inhibited rAAV2 entry into HeLa cells but did not affect viral transduction. Similarly, the macropinocytosis drug EIPA blocked viral entry into HEK293 cells without affecting transduction (23). Likewise, another study found that a powerful dominant negative genetic regulator of the clathrin-mediated endocytosis pathway could only partially inhibit rAAV2 transduction of HeLa cells (~50% inhibition) (19). In considering the present studies, our data uniquely draw together the seemingly disparate results from pre-

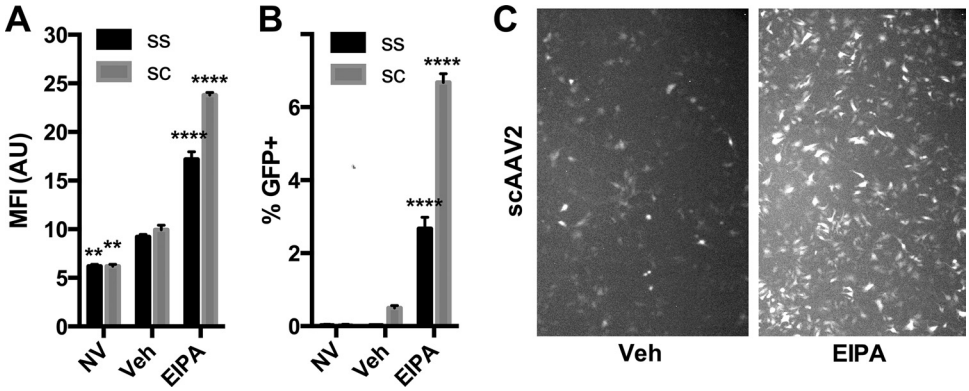

FIG 6 Macropinocytosis inhibitors enhance AAV transduction of HepG2 cells independent of effects on second-strand synthesis. Single-stranded (SS) AAV2-CMV-GFP, 1e5 vg, or self-complementary (SC) AAV2-CMV-GFP, 1e3 vg (or no virus [NV]), was delivered to HepG2 cells incubating in EIPA (10 μM) or a vehicle. Eighteen hours later, cells were analyzed by flow cytometry for GFP mean fluorescence intensity (MFI) (A) and percent GFP-positive cells (B). Representative photomicrographs of scAAV2 GFP expression with and without EIPA (C) were captured using a fluorescence microscope immediately prior to cell dissociation, using identical capture settings. Error bars represent standard errors. Statistical significance was determined using ANOVA (Dunnett's multiple-comparison test), comparing EIPA- and NV-treated groups to the vehicle- and virus-treated group. **, $P < 0.01$; ****, $P < 0.0001$.

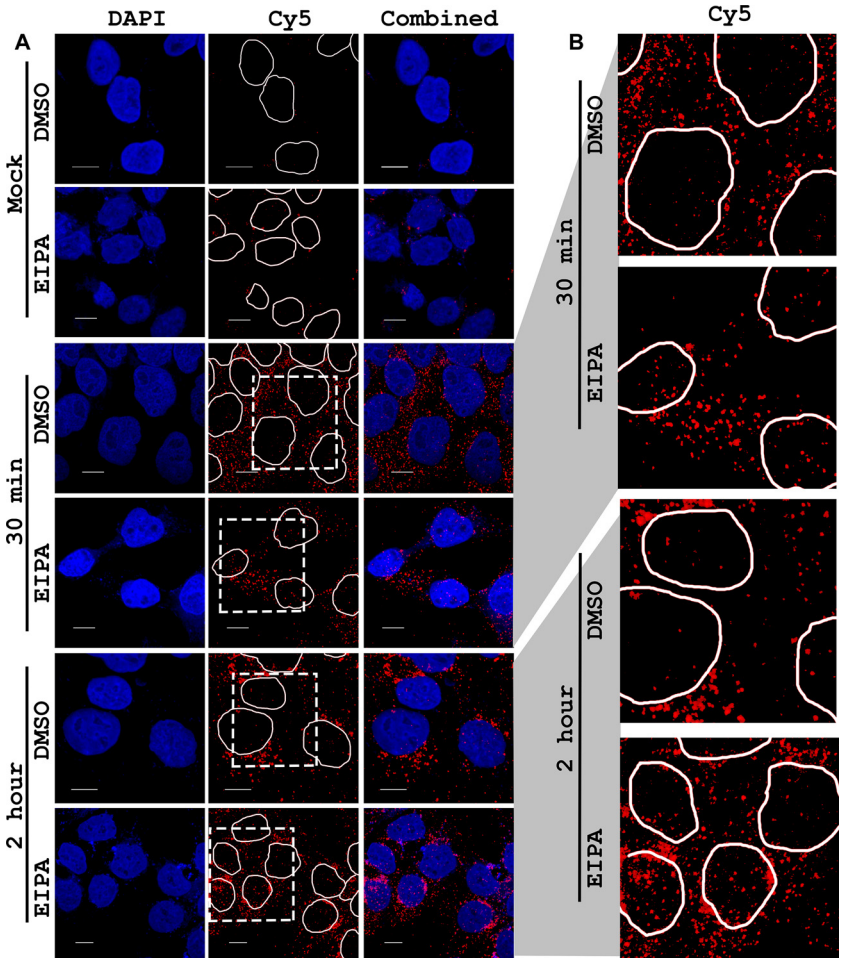

FIG 7 Effect of EIPA on trafficking of AAV2 in HepG2 cells. HepG2 cells were given ice-cold medium containing 1e5 vg of Cy5-labeled AAV2 (or no virus for mock-treated cells) and incubated at 4°C for 1 h, after which virus-containing medium was removed and replaced with warmed medium containing vehicle or 10 μM EIPA. After the designated time (30 min or 2 h), cells were paraformaldehyde fixed and mounted onto slides using a DAPI-containing mounting medium. Photomicrographs were captured on a confocal microscope. (A) DAPI channel, Cy5 channel (with DAPI-stained nuclei circled), and combined DAPI and Cy5 channels in columns. (B) The dashed outline region of the Cy5 channel of virus-treated cells (A) was scaled larger so that intranuclear Cy5-AAV could be more easily visualized. Scale bars represent 10 μm.

vious research in the field. For instance, our observed effect of EIPA inhibiting HeLa transduction by rAAV2 was noted previously by one group (23), whereas inhibition of the same by cytochalasin D was noted by another (21). Thus, the present data may provide the starting point for a unified theory of rAAV transduction in cells, which is inclusive of previous discoveries and is predicated on a new concept for rAAV trafficking: divergent infectious pathways of the virus between cells.

Our findings from three different macropinocytosis-related inhibitors—cytochalasin D, EIPA, and ML141—support the macropinocytosis-related pathway as playing a significant role in rAAV transduction of HeLa cells, across multiple rAAV serotypes. While there are limitations to our interpretation of EIPA as an inhibitor of viral transduction in these cells due to a decrease in transfected plasmid expression, these data support previous findings of macropinocytosis-based processes involved in HeLa cell rAAV trafficking (21), without ruling out the possibility of complementary clathrin-mediated or CLIC/GEEC pathway involvement in transduction. Perhaps the more novel aspect of this study, however, is that infectious entry of rAAV into hepatocellular lines HepG2 and Huh7 is substantially bolstered by macropinocytosis inhibition. The finding does not appear to be serotype specific, as the same relative enhancing effects were seen regardless of rAAV capsid (despite there being a substantial absolute difference in transduction of cells depending on virus encapsidation). We were able to replicate the transduction-enhancing effects of pharmacological inhibitors on HepG2 cells by knocking down a key effector protein, PAK1, in these cells. Not only did this genetic manipulation support our drug-related findings but also, taken in conjunction with the effects of CDC42 inhibition, it may begin to outline an active but nonproductive rAAV entry/trafficking pathway in certain cells.

As the effect of the macropinocytosis-inhibiting drugs was augmentative to rAAV transduction in hepatocellular lines, the chemical inhibitors might be seen as inducing a homeostatic effect of upregulating another viral entry pathway when a particular entry pathway is shut down. Such a phenomenon of shifted endocytosis pathways in cells has been previously proposed (60), based on the observation that inhibition of a clathrin-mediated entry pathway leads to upregulation of a pinocytic one. Such a mechanism may be necessary to maintain an exchange of solutes with the extracel-

lular milieu, and viral uptake patterns may be affected as a consequence of this homeostatic shift. Compensatory upregulation of an alternative entry pathway that is either more or less efficient for infectious entry suggests the possibility for multiple infectious pathways and/or for variability in transduction success garnered from a given pathway. Macropinocytosis may be an inefficient transduction pathway for rAAV in hepatocyte-like cells, and the blocking of this inefficient route may prevent viral entry via the inefficient pathway while upregulating another more "transduction-efficient" rAAV internalization pathway(s), such as the clathrin-mediated or CLIC/GEEC pathway.

Fitting with our *in vitro* hepatocellular transduction data, we observed *in vivo* liver transduction enhancement by rAAV2 found using either cytochalasin D or EIPA. The ability of these drugs to lead to increased transduction in such a complex system in such a preliminary study is highly encouraging for the use of similar, refined augmentation strategies relying on manipulation of early entry processes. While rAAV2 transduction in the liver was augmented up to 4-fold, it was interesting to note no difference in the total viral genomes found in liver tissue using either drug. In line with the possibility of competing viral entry pathways, it would be interesting for future studies to determine the nature of the liver-based virions: i.e., whether the virions are intact and trapped at a particular stage of trafficking. Importantly, not only did we observe enhancement of liver transduction by rAAV2, paralleling that of hepatocyte-like cell lines in culture, but also we found an inhibitory effect of EIPA on heart transduction. This demonstrates that the macropinocytosis inhibitor's effect on rAAV transduction *in vivo* is cell and tissue specific and thus that the manipulation of rAAV entry and early trafficking can be used as a strategy to increase precision in tissue targeting. Follow-up studies are under way to test whether other tissues (e.g., muscle, brain, and retina via direct delivery) are also differentially responsive to drugs targeting early viral entry pathways.

In conclusion, our study has demonstrated for the first time that the inhibition of an rAAV entry pathway can be conducive to higher-efficiency rAAV transduction in the cell. Further, we have shown that infectious entry pathways can differ dramatically between host cells, providing a key branch point for interpreting viral trafficking mechanisms and offering the potential for unification between seemingly disparate findings across model cells and organisms. Lastly, our proof-of-concept *in vivo* studies show promise that viral entry pathways are targets for improving rAAV delivery. Thus, our studies provide evidence for a novel means of controlling rAAV delivery and enhancing specificity and transduction efficiency, an approach that should allow for reduction in vector load and potentially improve clinical safety and efficacy for rAAV gene therapy.

ACKNOWLEDGMENTS

This work was supported by National Institutes of Health grants R01AI072176, R01AR064369, R01DK084033, P01HL1127611 (R.J.S.), and F32NS070356 (M.S.W.).

We thank Matthew Hirsch for technical assistance in performing Southern blotting and thank Jayme Warischalk, Thomas Lentz, and Robert Tarran for helpful advice and reagents. Equipment and software from the UNC Flow Cytometry Core, UNC Microscopy Services Laboratory, UNC Animal Clinical Chemistry Core, and the UNC Small Animal Imaging Facility were used in this study.

REFERENCES

1. **Mitchell AM, Nicolson SC, Warischalk JK, Samulski RJ.** 2010. AAV's anatomy: roadmap for optimizing vectors for translational success. Curr. Gene Ther. **10:**319–340. http://dx.doi.org/10.2174/156652310793180706.
2. **Manno CS, Arruda VR, Pierce GF, Glader B, Ragni M, Rasko J, Ozelo MC, Hoots K, Blatt P, Konkle B, Dake M, Kaye R, Razavi M, Zajko A, Zehnder J, Nakai H, Chew A, Leonard D, Wright JF, Lessard RR, Sommer JM, Tigges M, Sabatino D, Luk A, Jiang H, Mingozzi F, Couto L, Ertl HC, High KA, Kay MA.** 2006. Successful transduction of liver in hemophilia by AAV-factor IX and limitations imposed by the host immune response. Nat. Med. **12:**342–347. http://dx.doi.org/10.1038/nm1358.
3. **He Y, Weinberg MS, Hirsch M, Johnson MC, Tisch R, Samulski RJ, Li C.** 2013. Kinetics of adeno-associated virus serotype 2 (AAV2) and AAV8 capsid antigen presentation in vivo are identical. Hum. Gene Ther. **24:**545–553. http://dx.doi.org/10.1089/hum.2013.065.
4. **Nathwani AC, Tuddenham EGD, Rangarajan S, Rosales C, McIntosh J, Linch DC, Chowdary P, Riddell A, Pie AJ, Harrington C, O'Beirne J, Smith K, Pasi J, Glader B, Rustagi P, Ng CYC, Kay MA, Zhou J, Spence Y, Morton CL, Allay J, Coleman J, Sleep S, Cunningham JM, Srivastava D, Basner-Tschakarjan E, Mingozzi F, High KA, Gray JT, Reiss UM, Nienhuis AW, Davidoff AM.** 2011. Adenovirus-associated virus vector-mediated gene transfer in hemophilia B. N. Engl. J. Med. **365:**2357–2365. http://dx.doi.org/10.1056/NEJMoa1108046.
5. **Chao H.** 2000. Several log increase in therapeutic transgene delivery by distinct adeno-associated viral serotype vectors. Mol. Ther. **2:**619–623. http://dx.doi.org/10.1006/mthe.2000.0219.
6. **Davidson BL, Stein CS, Heth JA, Martins I, Kotin RM, Derksen TA, Zabner J, Ghodsi A, Chiorini JA.** 2000. Recombinant adeno-associated virus type 2, 4, and 5 vectors: transduction of variant cell types and regions in the mammalian central nervous system. Proc. Natl. Acad. Sci. U. S. A. **97:**3428–3432. http://dx.doi.org/10.1073/pnas.97.7.3428.
7. **Sipo I, Fechner H, Pinkert S, Suckau L, Wang X, Weger S, Poller W.** 2007. Differential internalization and nuclear uncoating of self-complementary adeno-associated virus pseudotype vectors as determinants of cardiac cell transduction. Gene Ther. **14:**1319–1329. http://dx.doi.org/10.1038/sj.gt.3302987.
8. **Bowles DE, McPhee SW, Li C, Gray SJ, Samulski JJ, Camp AS, Li J, Wang B, Monahan PE, Rabinowitz JE, Grieger JC, Govindasamy L, Agbandje-McKenna M, Xiao X, Samulski RJ.** 2012. Phase 1 gene therapy for Duchenne muscular dystrophy using a translational optimized AAV vector. Mol. Ther. **20:**443–455. http://dx.doi.org/10.1038/mt.2011.237.
9. **Asokan A, Conway JC, Phillips JL, Li C, Hegge J, Sinnott R, Yadav S, DiPrimio N, Nam H-J, Agbandje-McKenna M, McPhee S, Wolff J, Samulski RJ.** 2010. Reengineering a receptor footprint of adeno-associated virus enables selective and systemic gene transfer to muscle. Nat. Biotechnol. **28:**79–82. http://dx.doi.org/10.1038/nbt.1599.
10. **Petrs-Silva H, Dinculescu A, Li Q, Min S-H, Chiodo V, Pang J-J, Zhong L, Zolotukhin S, Srivastava A, Lewin AS, Hauswirth WW.** 2009. High-efficiency transduction of the mouse retina by tyrosine-mutant AAV serotype vectors. Mol. Ther. **17:**463–471. http://dx.doi.org/10.1038/mt.2008.269.
11. **Li C, DiPrimio N, Bowles DE, Hirsch ML, Monahan PE, Asokan A, Rabinowitz J, Agbandje-McKenna M, Samulski RJ.** 2012. Single amino acid modification of adeno-associated virus capsid changes transduction and humoral immune profiles. J. Virol. **86:**7752–7759. http://dx.doi.org/10.1128/JVI.00675-12.
12. **Li W, Asokan A, Wu Z, Van Dyke T, DiPrimio N, Johnson S J, Govindaswamy L, Agbandje-McKenna M, Leichtle S, Eugene Redmond J, McCown DTJ, Petermann KB, Sharpless NE, Samulski RJ.** 2008. Engineering and selection of shuffled AAV genomes: a new strategy for producing targeted biological nanoparticles. Mol. Ther. **16:**1252–1260. http://dx.doi.org/10.1038/mt.2008.100.
13. **Koerber JT, Maheshri N, Kaspar BK, Schaffer DV.** 2006. Construction of diverse adeno-associated viral libraries for directed evolution of enhanced gene delivery vehicles. Nat. Protoc. **1:**701–706. http://dx.doi.org/10.1038/nprot.2006.93.
14. **Zhong L, Zhao W, Wu J, Li B, Zolotukhin S, Govindasamy L, Agbandje-McKenna M, Srivastava A.** 2007. A dual role of EGFR protein tyrosine kinase signaling in ubiquitination of AAV2 capsids and viral second-strand DNA Synthesis. Mol. Ther. **15:**1323–1330. http://dx.doi.org/10.1038/sj.mt.6300170.

15. **Duan D, Yue Y, Yan Z, Yang J, Engelhardt JF.** 2000. Endosomal processing limits gene transfer to polarized airway epithelia by adeno-associated virus. J. Clin. Invest. **105:**1573–1587. http://dx.doi.org/10.1172/JCI8317.
16. **Johnson JS, Li C, DiPrimio N, Weinberg MS, McCown TJ, Samulski RJ.** 2010. Mutagenesis of adeno-associated virus type 2 capsid protein VP1 uncovers new roles for basic amino acids in trafficking and cell-specific transduction. J. Virol. **84:**8888–8902. http://dx.doi.org/10.1128/JVI.00687-10.
17. **McCarty DM, Monahan PE, Samulski RJ.** 2001. Self-complementary recombinant adeno-associated virus (scAAV) vectors promote efficient transduction independently of DNA synthesis. Gene Ther. **8:**1248–1254. http://dx.doi.org/10.1038/sj.gt.3301514.
18. **Wu Z, Sun J, Zhang T, Yin C, Yin F, Van Dyke T, Samulski RJ, Monahan PE.** 2008. Optimization of self-complementary AAV vectors for liver-directed expression results in sustained correction of hemophilia B at low vector dose. Mol. Ther. **16:**280–289. http://dx.doi.org/10.1038/sj.mt.6300355.
19. **Bartlett JS, Wilcher R, Samulski RJ.** 2000. Infectious entry pathway of adeno-associated virus and adeno-associated virus vectors. J. Virol. **74:**2777–2785. http://dx.doi.org/10.1128/JVI.74.6.2777-2785.2000.
20. **Duan D, Li Q, Kao AW, Yue Y, Pessin JE, Engelhardt JF.** 1999. Dynamin is required for recombinant adeno-associated virus type 2 infection. J. Virol. **73:**10371–10376.
21. **Sanlioglu S, Benson PK, Yang J, Atkinson EM, Reynolds T, Engelhardt JF.** 2000. Endocytosis and nuclear trafficking of adeno-associated virus type 2 are controlled by Rac1 and phosphatidylinositol-3 kinase activation. J. Virol. **74:**9184–9196. http://dx.doi.org/10.1128/JVI.74.19.9184-9196.2000.
22. **Douar AM, Poulard K, Stockholm D, Danos O.** 2001. Intracellular trafficking of adeno-associated virus vectors: routing to the late endosomal compartment and proteasome degradation. J. Virol. **75:**1824–1833. http://dx.doi.org/10.1128/JVI.75.4.1824-1833.2001.
23. **Nonnenmacher M, Weber T.** 2011. Adeno-associated virus 2 infection requires endocytosis through the CLIC/GEEC pathway. Cell Host Microbe **10:**563–576. http://dx.doi.org/10.1016/j.chom.2011.10.014.
24. **Schulz WL, Haj AK, Schiff LA.** 2012. Reovirus uses multiple endocytic pathways for cell entry. J. Virol. **86:**12665–12675. http://dx.doi.org/10.1128/JVI.01861-12.
25. **Boisvert M, Fernandes S, Tijssen P.** 2010. Multiple pathways involved in porcine parvovirus cellular entry and trafficking toward the nucleus. J. Virol. **84:**7782–7792. http://dx.doi.org/10.1128/JVI.00479-10.
26. **Bantel-Schaal U, Braspenning-Wesch I, Kartenbeck J.** 2009. Adeno-associated virus type 5 exploits two different entry pathways in human embryo fibroblasts. J. Gen. Virol. **90:**317–322. http://dx.doi.org/10.1099/vir.0.005595-0.
27. **Frampton AR, Stolz DB, Uchida H, Goins WF, Cohen JB, Glorioso JC.** 2007. Equine herpesvirus 1 enters cells by two different pathways, and infection requires the activation of the cellular kinase ROCK1. J. Virol. **81:**10879–10889. http://dx.doi.org/10.1128/JVI.00504-07.
28. **Acosta EG, Castilla V, Damonte EB.** 2009. Alternative infectious entry pathways for dengue virus serotypes into mammalian cells. Cell. Microbiol. **11:**1533–1549. http://dx.doi.org/10.1111/j.1462-5822.2009.01345.x.
29. **Nicolson SC, Samulski RJ.** 2014. Recombinant adeno-associated virus utilizes host cell nuclear import machinery to enter the nucleus. J. Virol. **88:**4132–4144. http://dx.doi.org/10.1128/JVI.02660-13.
30. **Grieger JC, Choi VW, Samulski RJ.** 2006. Production and characterization of adeno-associated viral vectors. Nat. Protoc. **1:**1412–1428. http://dx.doi.org/10.1038/nprot.2006.207.
31. **Weinberg MS, Blake BL, Samulski RJ, McCown TJ.** 2011. The influence of epileptic neuropathology and prior peripheral immunity on CNS transduction by rAAV2 and rAAV5. Gene Ther. **18:**961–968. http://dx.doi.org/10.1038/gt.2011.49.
32. **Xiao PJ, Samulski RJ.** 2012. Cytoplasmic trafficking, endosomal escape, and perinuclear accumulation of adeno-associated virus type 2 particles are facilitated by microtubule network. J. Virol. **86:**10462–10473. http://dx.doi.org/10.1128/JVI.00935-12.
33. **Heikkilä O, Susi P, Tevaluoto T, Harma H, Marjomaki V, Hyypia T, Kiljunen S.** 2010. Internalization of coxsackievirus A9 is mediated by 2-microglobulin, dynamin, and Arf6 but not by caveolin-1 or clathrin. J. Virol. **84:**3666–3681. http://dx.doi.org/10.1128/JVI.01340-09.
34. **Mitchell AM, Li C, Samulski RJ.** 2013. Arsenic trioxide stabilizes accumulations of adeno-associated virus virions at the perinuclear region, increasing transduction in vitro and in vivo. J. Virol. **87:**4571–4583. http://dx.doi.org/10.1128/JVI.03443-12.
35. **El-Sayed A, Harashima H.** 2013. Endocytosis of gene delivery vectors: from clathrin-dependent to lipid raft-mediated endocytosis. Mol. Ther. **21:**1118–1130. http://dx.doi.org/10.1038/mt.2013.54.
36. **Elliott G, O'Hare P.** 1997. Intercellular trafficking and protein delivery by a herpesvirus structural protein. Cell **88:**223–233. http://dx.doi.org/10.1016/S0092-8674(00)81843-7.
37. **Wang K, Huang S, Kapoor-Munshi A, Nemerow G.** 1998. Adenovirus internalization and infection require dynamin. J. Virol. **72:**3455–3458.
38. **Gustin KE, Sarnow P.** 2001. Effects of poliovirus infection on nucleo-cytoplasmic trafficking and nuclear pore complex composition. EMBO J. **20:**240–249. http://dx.doi.org/10.1093/emboj/20.1.240.
39. **Westerink WM, Schoonen WG.** 2007. Phase II enzyme levels in HepG2 cells and cryopreserved primary human hepatocytes and their induction in HepG2 cells. Toxicol. In Vitro **21:**1592–1602. http://dx.doi.org/10.1016/j.tiv.2007.06.017.
40. **Nakabayashi H, Taketa K, Miyano K, Yamane T, Sato J.** 1982. Growth of human hepatoma cells lines with differentiated functions in chemically defined medium. Cancer Res. **42:**3858–3863.
41. **Kern A, Schmidt K, Leder C, Muller OJ, Wobus CE, Bettinger K, Von der Lieth CW, King JA, Kleinschmidt JA.** 2003. Identification of a heparin-binding motif on adeno-associated virus type 2 capsids. J. Virol. **77:**11072–11081. http://dx.doi.org/10.1128/JVI.77.20.11072-11081.2003.
42. **Koivusalo M, Welch C, Hayashi H, Scott CC, Kim M, Alexander T, Touret N, Hahn KM, Grinstein S.** 2010. Amiloride inhibits macropinocytosis by lowering submembranous pH and preventing Rac1 and Cdc42 signaling. J. Cell Biol. **188:**547–563. http://dx.doi.org/10.1083/jcb.200908086.
43. **Knowles MR, Church NL, Waltner WE, Yankaskas JR, Gilligan P, King M, Edwards LJ, Helms RW, Boucher RC.** 1990. A pilot study of aerosolized amiloride for the treatment of lung disease in cystic fibrosis. N. Engl. J. Med. **322:**1189–1194. http://dx.doi.org/10.1056/NEJM199004263221704.
44. **Richardson A, Bayliss J, Scriven AJ, Parameshwar J, Poole-Wilson PA, Sutton GC.** 1987. Double-blind comparison of captopril alone against frusemide plus amiloride in mild heart failure. Lancet **ii:**709–711.
45. **Hofmann T, Senier I, Bittner P, Huls G, Schwandt HJ, Lindemann H.** 1997. Aerosolized amiloride: dose effect on nasal bioelectric properties, pharmacokinetics, and effect on sputum expectoration in patients with cystic fibrosis. J. Aerosol Med. **10:**147–158. http://dx.doi.org/10.1089/jam.1997.10.147.
46. **Pons G, Marchand MC, d'Athis P, Sauvage E, Foucard C, Chaumet-Riffaud P, Sautegeau A, Navarro J, Lenoir G.** 2000. French multicenter randomized double-blind placebo-controlled trial on nebulized amiloride in cystic fibrosis patients. The Amiloride-AFLM Collaborative Study Group. Pediatr. Pulmonol. **30:**25–31. http://dx.doi.org/10.1002/1099-0496(200007)30:1<25::AID-PPUL5>3.0.CO;2-C.
47. **Bondarava M, Li T, Endl E, Wehner F.** 2009. α-ENaC is a functional element of the hypertonicity-induced cation channel in HepG2 cells and it mediates proliferation. Pflugers Arch. **458:**675–687. http://dx.doi.org/10.1007/s00424-009-0649-z.
48. **Baldini PM, De Vito P, Vismara D, Bagni C, Zalfa F, Minieri M, Di Nardo P.** 2005. Atrial natriuretic peptide effects on intracellular pH changes and ROS production in HEPG2 cells: role of p38 MAPK and phospholipase D. Cell. Physiol. Biochem. **15:**77–88. http://dx.doi.org/10.1159/000083640.
49. **Kolyada AY, Lebedeva TV, Johns CA, Madias NE.** 1994. Proximal regulatory elements and nuclear activities required for transcription of the human Na+/H+ exchanger (NHE-1) gene. Biochim. Biophys. Acta **1217:**54–64. http://dx.doi.org/10.1016/0167-4781(94)90124-4.
50. **Masereel B, Pochet L, Laeckmann D.** 2003. An overview of inhibitors of Na(+)/H(+) exchanger. Eur. J. Med. Chem. **38:**547–554. http://dx.doi.org/10.1016/S0223-5234(03)00100-4.
51. **Lee C, Tannock I.** 1996. Pharmacokinetic studies of amiloride and its analogs using reversed-phase high-performance liquid chromatography. J. Chromatogr. B Biomed. Appl. **685:**151–157. http://dx.doi.org/10.1016/0378-4347(96)00158-2.
52. **Maidorn RP, Cragoe EJ, Jr, Tannock IF.** 1993. Therapeutic potential of analogues of amiloride: inhibition of the regulation of intracellular pH as a possible mechanism of tumour selective therapy. Br. J. Cancer **67:**297–303. http://dx.doi.org/10.1038/bjc.1993.56.
53. **Ponnazhagan S, Mukherjee P, Yoder MC, Wang XS, Zhou SZ, Kaplan J, Wadsworth S, Srivastava A.** 1997. Adeno-associated virus 2-mediated

gene transfer in vivo: organ-tropism and expression of transduced sequences in mice. Gene **190:**203–210. http://dx.doi.org/10.1016/S0378-1119(96)00576-8.

54. **Kozma R, Ahmed S, Best A, Lim L.** 1995. The Ras-related protein Cdc42Hs and bradykinin promote formation of peripheral actin microspikes and filopodia in Swiss 3T3 fibroblasts. Mol. Cell. Biol. **15:**1942–1952.
55. **Cox D, Chang P, Zhang Q, Reddy PG, Bokoch GM, Greenberg S.** 1997. Requirements for both Rac1 and Cdc42 in membrane ruffling and phagocytosis in leukocytes. J. Exp. Med. **186:**1487–1494. http://dx.doi.org/10.1084/jem.186.9.1487.
56. **Dharmawardhane S, Schurmann A, Sells MA, Chernoff J, Schmid SL, Bokoch GM.** 2000. Regulation of macropinocytosis by p21-activated kinase-1. Mol. Biol. Cell **11:**3341–3352. http://dx.doi.org/10.1091/mbc.11.10.3341.
57. **Amstutz B, Gastaldelli M, Kalin S, Imelli N, Boucke K, Wandeler E, Mercer J, Hemmi S, Greber UF.** 2008. Subversion of CtBP1-controlled macropinocytosis by human adenovirus serotype 3. EMBO J. **27:**956–969. http://dx.doi.org/10.1038/emboj.2008.38.
58. **Kälin S, Amstutz B, Gastaldelli M, Wolfrum N, Boucke K, Havenga M, DiGennaro F, Liska N, Hemmi S, Greber UF.** 2010. Macropinocytotic uptake and infection of human epithelial cells with species B2 adenovirus type 35. J. Virol. **84:**5336–5350. http://dx.doi.org/10.1128/JVI.02494-09.
59. **Ju XD, Lou SQ, Wang WG, Peng JQ, Tian H.** 2004. Effect of hydroxyurea and etoposide on transduction of human bone marrow mesenchymal stem and progenitor cell by adeno-associated virus vectors. Acta Pharmacol. Sin. **25:**196–202.
60. **Damke H, Baba T, van der Bliek AM, Schmid SL.** 1995. Clathrin-independent pinocytosis is induced in cells overexpressing a temperature-sensitive mutant of dynamin. J. Cell Biol. **131:**69–80. http://dx.doi.org/10.1083/jcb.131.1.69.